Sigma Journal of Engineering and Natural Sciences
Web page info: https://sigma.yildiz.edu.tr
DOI: 10.14744/sigma.2024.00053

Research Article

Phase-mismatch third harmonic generation in quantum magnetoplasma

Shiv SINGH[1], Abhisek Kumar SINGH[2,*], Punit KUMAR[3]

[1]*Department of Physics, Babu Banarasi Das University, Lucknow, 226028, India*
[2]*Department of Physics, G L Bajaj Group of Institutions, Mathura, 281406, India*
[3]*Department of Physics, University of Lucknow, Lucknow, 226007, India*

ARTICLE INFO

Article history
Received: 14 January 2024
Revised: 11 March 2024
Accepted: 15 April 2024

Keywords:
Electron Spin-1/2; Harmonic Generation; QHD Model; Quantum Diffraction Effects; Quantum Plasma

ABSTRACT

An analytical theory is developed for studying the phenomenon of generation of third harmonic radiation by the propagation of circularly polarized laser beam in homogenous underdense quantum magnetoplasma by using recently developed Quantum hydrodynamic (QHD) model. The effects of quantum Bohm potential, quantum statistical Fermi pressure and electron spin -1/2 have been taken into account. A circularly polarized laser beam propagating through quantum plasma produces density oscillations at second harmonic. The density oscillation combined with the oscillatory velocity produces third order current density, which derives third order harmonic radiation. The field amplitude of third harmonic radiation with reference to the fundamental amplitude of the incident circularly polarized radiation and the conversion efficiency for wave number-mismatch has been analyzed. It is observed that the efficiency of generated third harmonic is affected significantly due to the magnetic field strength, plasma electron density, intensity of circularly polarized laser pulse and quantum diffraction effects.

Cite this article as: Singh S, Singh AK, Kumar P. Phase-mismatch third harmonic generation in quantum magnetoplasma. Sigma J Eng Nat Sci 2025;43(2):400–407.

INTRODUCTION

Over the past three decades, the investigation into the interaction of high-intensity laser pulses with plasma, leading to harmonic generation, has been a dynamic and evolving field [1]. The intricate interplay between intense laser pulses and plasma gives rise to a plethora of parametric instabilities and nonlinear phenomena. These encompass laser wakefield acceleration, inertial confinement fusion, Raman scattering, self-phase modulation, ponderomotive self-focusing, and harmonic radiation generation. The generation of harmonic radiation within both laser-produced and laboratory plasmas is a pivotal subject, offering substantial potential for plasma diagnostics [2-8]. In recent years, significant attention has been directed towards understanding second and third harmonic generation within laser-produced plasmas [9-11].

The harmonic generation process involves the combination of two photons with energies E_1 and E_1, along with momenta k_1 and k_2, resulting in the creation of a photon with energy E_3 and momentum k_3. Here, ω_1 and k_1 represent the frequency and wave vector of the fundamental

*Corresponding author.
*E-mail address: abhisek.singh@glbajajgroup.org , abhisheklu99@gmail.com

This paper was recommended for publication in revised form by Editor-in-Chief Ahmet Selim Dalkilic

wave, while ω_2 and k_2 correspond to the frequency and wave vector of the second harmonic wave, adhering to the dispersion relation for electromagnetic waves. During the phenomenon of third harmonic generation, the fundamental laser beam generates a beam at a frequency three times that of the fundamental frequency. In the context of circularly polarized intense laser interaction with a homogeneous plasma, a transverse nonlinear plasma current is induced, giving rise to the generation of odd harmonics of the laser frequency in the forward direction [12]. Although there have been analyses of high-order harmonic generation [13-14], the phenomenon of third harmonic generation [15-17] holds a distinct and significant place within the realm of laser-plasma interactions.

Prior research efforts have primarily focused on classical plasma behavior. However, when examining plasmas where the de Broglie thermal wavelength of charge carriers becomes comparable to or exceeds the inter-particle distance, or when the temperature T approaches or falls below the electron Fermi temperature, a state of degeneracy emerges. This introduces the influence of Fermi-Dirac distribution on plasma particles, leading to quantum degeneracy effects becoming significant. This shift towards quantum behavior prompts the investigation of quantum plasma phenomena. Over the past decade, there has been a growing interest in exploring novel aspects of quantum plasma due to its valuable applications in nanoscale and nanoelectronic devices [18,19], its relevance in superdense astrophysical entities [20-24], and its involvement in phenomena like quantum plasma echoes [25], quantum x-ray free electron lasers [26], and intense laser-solid density plasma experiments [27-31]. Multiple studies have delved into harmonic generation within quantum magnetoplasmas [32-36], with some focusing on phase-matched third harmonic generation of laser pulses in highly dense quantum plasmas under the influence of wiggler magnetic fields [37]. However, it is important to note that, to the best of our knowledge, no prior research has attempted to explore the phenomenon of phase-mismatched third harmonic generation induced by circularly polarized lasers in densely magnetized quantum plasmas while accounting for the effects of electron spin-1/2. Phase mismatch in harmonics of plasma waves refers to the discrepancy between the ideal phase relationships of different harmonic components within a plasma wave. This phenomenon arises due to non-linear interactions among plasma particles, causing the harmonics to oscillate out of sync with each other. In plasma machines and reactors, understanding and controlling phase mismatch in harmonics is crucial for optimizing performance and stability. For instance, in fusion reactors, where plasma waves play a key role in confining and heating the plasma, phase mismatch can lead to inefficient energy transfer and reduced fusion yield.

Researchers and engineers utilize various techniques to mitigate phase mismatch, such as adjusting the plasma parameters, designing specialized waveguides or resonant cavities and implementing feedback control systems. By minimizing phase mismatch, plasma devices can achieve more efficient energy conversion, enhanced confinement, and improved overall performance, contributing to advancements in fields such as energy production, materials processing, and space propulsion.

The primary objective of this research is to conduct a comprehensive analytical investigation into the generation of phase mismatch third harmonic radiation through circularly polarized laser interaction with a high-density, low-temperature quantum plasma. This study focuses on the assumption of a cold plasma, enabling the disregard of electron thermal motion. Employing a mildly relativistic framework, the research employs a perturbative approach along with a recently developed Quantum Hydrodynamic (QHD) model. The QHD model extends the classical plasma model by formulating transport equations based on the conservation principles of particles, momentum, and energy. Noteworthy advantages of the QHD model compared to kinetic models include its computational efficiency, utilization of relevant macroscopic variables like momentum and energy, and straightforward implementation of boundary conditions. This model facilitates the examination of nonlinear phenomena, making it a preferable choice for describing such occurrences in quantum plasma [38, 39]. Within the mildly relativistic regime, relativistic effects become pronounced in higher-order velocity components and magnitudes. This paper is organized as follows. It is divided into four sections. Sec. 2 is devoted to nonlinear current density of third harmonic radiation generation and conversion efficiency has been analyzed in sec. 3. Finally, Sec. 4 devoted with summary and conclusion of the work.

Source Current

Let us take the propagation of a circularly polarized laser pulse of frequency ω_0 and wave number k_0 and constant amplitude E_0 in magnetized cold quantum plasma of uniform density n_0 along the direction of static magnetic field $B_z \,||\, \hat{z}$. The fields of laser are

$$\vec{E}_{(x,y)} = E_0\left(\hat{x} + i\hat{y}\right)e^{i(k_0 z - \omega t)} + c.c. \tag{1}$$

and

$$\vec{B}_{(x,y)} = c\vec{k}_0 \times \vec{E}_{(x,y)} \big/ \omega_0 + c.c.$$

We assume that the plasma is cold and there is a fixed ionic background to ensure charge neutrality and fast processes to be considered in quantum plasma. Response of electron to the electromagnetic field is governed by the set of QHD equations [34, 40],

$$\frac{\partial(\gamma\vec{v})}{\partial t} = -\frac{e}{m\gamma}\left[\vec{E} + \frac{1}{c}(\vec{v}\times\vec{B})\right] - \frac{v_F^2}{3n_0^2}\frac{\nabla n^3}{n} + \frac{\hbar^2}{2m^2\gamma^2}\nabla\left(\frac{1}{\sqrt{n}}\nabla^2\sqrt{n}\right) - \frac{2\mu_B}{m\hbar}\vec{S}.(\nabla\vec{B}), \quad (2)$$

$$\frac{\partial\vec{S}}{\partial t} = \frac{2\mu_B}{\hbar}(\vec{B}\times\vec{S}), \quad (3)$$

$$\frac{\partial(\gamma m)}{\partial t} + \nabla(\gamma m\vec{v}) = 0. \quad (4)$$

where, m is the rest mass of electron, e is the electron charge, n is the electron density, γ is the relativistic factor, $\hbar$ is Planck's constant divided by 2π, S is the spin angular momentum with $S_0 = |S_0| = \hbar/2$, $m_B = e\hbar/2m$ is the Bohr magneton and $v_F = (\hbar/m)(3\pi^2 n)^{1/3}$ represents the Fermi velocity of electrons. On the right hand side of equation (2) the first term represents the Lorentz force, second term is the electron Fermi pressure, third term is the quantum Bohm potential produced due to density fluctuations and the last term denotes the force due to spin magnetic moment of plasma electrons and the classical case may be recovered in the limit of $\hbar = 0$.

On perturbation of eqs. (2) and (4) in orders of radiation field, the first order quiver velocity and density components are found to

$$v_x^{(1)} = \frac{1}{\left(\omega_c^2 - \omega_0^2\right)}\left[\frac{ie(\omega_0 - \omega_c)}{m} + \frac{k_0 Q(i\omega_c n_{y1} - \omega_0 n_{x1})}{n_0} + \frac{2i\mu_B k_0 S_0(\omega_c - \omega_0)}{m\hbar}\right]E_0 e^{i(k_0 z - \omega_0 t)} + c.c., \quad (5)$$

$$v_y^{(1)} = \left[\frac{-e}{m\omega_0} + \frac{i\omega_c v_{x1}}{\omega_0} + \frac{k_0 n_{y1} Q}{n_0\omega_0} + \frac{2\mu_B k_0 S_0}{m\hbar\omega_0}\right]E_0 e^{i(k_0 z - \omega_0 t)} + c.c., \quad (6)$$

$$n_x^{(1)} = \frac{n_0 k}{\omega_0\left\{k_0^2 Q + \left(\omega_c^2 - \omega_0^2\right)\right\}}\left[\frac{ie(\omega_0 - \omega_c)}{m} + \frac{ik_0 Q\omega_c n_{y1}}{n_0} + \frac{2i\mu_B S_0 k_0(\omega_c - \omega_0)}{m\hbar}\right]E_0 e^{i(k_0 z - \omega_0 t)} + c.c. \quad (7)$$

$$n_y^{(1)} = \frac{n_0 k_0\left(\omega_c^2 - \omega_0^2\right)}{\left\{(\omega_0^2 - k_0^2)(\omega_c^2 - \omega_0^2) + k_0^2 Q\omega_c^2\right\}}\left[\frac{-e}{m} + \frac{e\omega_c}{m(\omega_c + \omega_0)} - \frac{ik_0 Q\omega_0\omega_c n_{x1}}{n_0(\omega_c^2 - \omega_0^2)} - \frac{2\omega_c\mu_B S_0 k_0}{m\hbar(\omega_c + \omega_0)} + \frac{2\mu_B S_0 k_0}{m\hbar}\right]E_0 e^{i(k_0 z - \omega_0 t)} + c.c. \quad (8)$$

Quantum degenerate plasma has a crucial characteristic called spin. It is essential for exposing the plasma to the external magnetic field, whose impact is discernible in the perturbed spin magnetic moment for plasma electrons via the spin angular momentum,

$$S_x^{(1)} = \frac{2i\mu_B S_0\left\{\frac{2b\mu_B}{\hbar} - \omega_0\right\}}{\hbar\left\{\frac{4b^2\mu_B^2}{\hbar^2} - \omega_0^2\right\}}E_0 e^{i(k_0 z - \omega_0 t)} + c.c., \quad (9)$$

$$S_y^{(1)} = \frac{-2\mu_B(bS_{x1} - iS_0)}{i\hbar\omega_0}E_0 e^{i(k_0 z - \omega_0 t)} + c.c \quad (10)$$

and

$$S_z^{(1)} = \frac{-2\mu_B S_0(1-i)}{\hbar\omega_0}E_0 e^{i(k_0 z - \omega_0 t)} + c.c. \quad (11)$$

By following similar steps for nth harmonic, the velocity, perturbed density and spin magnetic moment for electron can be obtained by substituting $\omega_0 \to n\omega_0$, $\vec{E}_0 \to \vec{E}_n$, $(k_0 z - \omega_0 t) \to (k_n z - n\omega_0 t)$, from equations (5)-(11). Hence, the linear part of induced current density for nth harmonic, $J^{(1)}(n\omega_0) = J_c^{(1)}(n\omega_0) + J_c^{(1)}(n\omega_0)$ can be written as,

$$J^{(1)}(n\omega_0) = \left[J_c^{(1)}(n\omega_0) + J_s^{(1)}(n\omega_0)\right]E_n e^{i(k_n z - n\omega_0 t)} + c.c. \quad (12)$$

where, $\vec{J}_c = -\frac{2\mu_B}{\hbar}\nabla(n.S)$ is the current density due to the spin magnetic moment and $\vec{J}_c = -e(\vec{n}.\vec{v})$ is the conventional current. The dispersion relation for nth harmonic is

Third Harmonic Generation

The laser produces oscillatory velocity of electrons and exerts a ponderomotive force $F_2 = -(1/2)e\vec{v}_1 \times B_1$ on them at $(2k_0, 2\omega_0)$, which gives rise to oscillatory velocity $v^{(2)}$, which couples with density perturbation at laser frequency through equation of continuity to produce density perturbation at $(2k_0, 2\omega_0)$ and $n^{(2)}$ couples with $v^{(1)}$ to produce nonlinear current density at the third harmonic of frequency. The third harmonic velocity and density components are obtained as,

$$v_x^{(3)} = \frac{1}{(\omega_c^2 - 9\omega_0^2)}\left[3\omega_0(3\omega_0 v_{x1} - i\omega_c v_{y1}) + \frac{iev_{z2}(\omega_c - 3\omega_0)}{mc} + \frac{2i\mu_B k_0}{m\hbar}(\omega_c S_{y2} - 3\omega_0 S_{X2})\right]E_0^3 e^{3i(k_0 z - \omega_0 t)} + c.c \quad (13)$$

$$v_y^{(3)} = \left[\frac{i\omega_c v_{x3}}{3\omega_0} + \frac{ev_{z2}}{3mc\omega_0} - v_{y1} + \frac{2\mu_B k_0 S_{y2}}{3m\hbar\omega_0}\right]E_0^3 e^{3i(k_0 z - \omega_0 t)} + c.c. \quad (14)$$

$$v_z^{(3)} = \left[\frac{ie}{3m\omega_0 c}(iv_{y2} - v_{x2})\right] E_0^3 e^{3i(k_0 z - \omega_0 t)} + c.c. \quad (15)$$

$$n_x^{(3)} = \frac{k_0}{\omega_0}\left[v_{x2}n_{x1} + v_{x1}n_{x2} + n_0 v_{x3}\right] E_0^3 e^{3i(k_0 z - \omega_0 t)} + c.c. \quad (16)$$

$$n_y^{(3)} = \frac{k_0}{\omega_0}\left[v_{y2}n_{y1} + v_{y1}n_{y2} + n_0 v_{y3}\right] E_0^3 e^{3i(k_0 z - \omega_0 t)} + c.c. \quad (17)$$

$$n_z^{(3)} = \frac{k_0}{\omega_0}\left[v_{z2}n_{z1} + v_{z1}n_{z2} + n_0 v_{z3}\right] E_0^3 e^{3i(k_0 z - \omega_0 t)} + c.c. \quad (18)$$

where,

$$v_{x2} = \left[\frac{2i\mu_B k_0(\omega_c S_{y1} - 2\omega_0 S_{x1})}{m\hbar(\omega_c^2 - 4\omega_0^2)}\right],\ v_{y2} = \left[\frac{i\omega_c v_{x2}}{2\omega_0} + \frac{\mu_B k_0 S_{y1}}{m\hbar\omega_0}\right],$$

$$v_{z2} = \left[\frac{-ie(v_{x1} - iv_{y1})}{2m\omega_0 c}\right],\ n_{x2} = \left[\frac{k_0 n_0 v_{x2}}{\omega_0} + \frac{k_0 n_{x1} v_{x1}}{\omega_0}\right],$$

$$n_{y2} = \left[\frac{k_0 n_0 v_{y2}}{\omega_0} + \frac{k_0 n_{y1} v_{y1}}{\omega_0}\right]$$

and

$$n_{z2} = \left[\frac{k_0 n_0 v_{z2}}{\omega_0} + \frac{k_0 n_{z1} v_{z1}}{\omega_0}\right].$$

The spin angular momenta also contributes to source current thus we need to evaluate the spin magnetic moment plasma electron at third harmonic,

$$S_x^{(3)} = \frac{2i\mu_B}{3\hbar\omega_0}(S_{z3} + iS_{z2}) E_0^3 e^{3i(k_0 z - \omega_0 t)} + c.c. \quad (19)$$

$$S_y^{(3)} = \frac{-2i\mu_B S_{z2}}{3\hbar\omega_0} E_0^3 e^{3i(k_0 z - \omega_0 t)} + c.c. \quad (20)$$

$$S_z^{(3)} = \frac{1}{\left(\frac{4\mu_B^2 b^2}{\hbar^2} - 9\omega_0^2\right)}\left[\frac{-4i\mu_B^2 b S_{z2}}{\hbar^2} + \frac{6i\mu_B\omega_0}{\hbar}(S_{y2} - iS_{x2})\right] E_0^3 e^{3i(k_0 z - \omega_0 t)} + c.c. \quad (21)$$

where,

$$S_{x2} = \frac{\left[\frac{2b\mu_B}{\hbar}\left\{\frac{2i\mu_B}{\hbar} + ik_0 s_{y1} v_{y1}\right\} - 2i\omega_0\left\{\frac{2\mu_B S_{z1}}{\hbar} - ik_0 v_{x1} S_{x1}\right\}\right]}{\left\{\frac{4\mu_B^2 b^2}{\hbar^2} - 4\omega_0^2\right\}},$$

$$S_{y2} = \left[\frac{ib\mu_B S_{x2}}{\hbar\omega_0} + \frac{\mu_B S_{z1}}{\hbar\omega_0} + \frac{k_0 S_{y1} v_{y1}}{2\omega_0}\right]$$

and

$$S_{z2} = \frac{i\mu_B(iS_{y1} - S_{x1})}{\hbar\omega_0}.$$

The third harmonic source current is

$$\vec{J}_{NL}^{(3)} = (J_{S3} + J_{c3})\mathrm{E}_0^3 e^{3i(k_0 z - \omega_0 t)} + c.c. \quad (22)$$

where, J_{S3} and J_{C3} are the magnetization due to spin effect of electron and conventional current density,

$$J_{S3} = -\frac{6ik_0\mu_B}{\hbar}\left[n_0 S_{x3} + S_0 n_{x3} + n_{x1}S_{x2} + n_{x2}S_{x1} + n_0 S_{y3} + S_0 n_{y3} + n_{y1}S_{y2} + n_{y2}S_{y1} + n_0 S_{z3} + S_0 n_{z3} + S_{z1}n_{z2} + S_{z2}n_{z1}\right]$$

and

$$J_{c3} = -e.\left[n_0 v_{x3} + n_{x1}v_{x2} + n_{x2}v_{x1} + n_0 v_{y3} + n_{y1}v_{y2} + n_{y2}v_{y1} + n_0 v_{z3} + n_{z2}v_{z1} + n_{z1}v_{z2}\right]$$

The dispersion relation for n[th] harmonic is

$$c^2 k_n^2 = n^2\omega_0^2 + \omega_p^2 \frac{imn\omega_0^2\left\{J_c^{(1)}(n\omega_0) + J_s^{(1)}(n\omega_0)\right\}}{n_0 e^2}. \quad (23)$$

The above equation reduces to well known dispersion relations for fundamental, second and third harmonic wave propagating in plasma in the absence of applied magnetic field. Here wave refractive indices corresponding to fundamental, second and third harmonics are $(\mu_1 = ck_1/\omega_0)$, $(\mu_2 = ck_2/\omega_0)$, and $(\mu_3 = ck_3/\omega_0)$.

Third Harmonic Efficiency

The non-linear component of the third source current $\vec{J}_{NL}^{(3)}$, can be used with the wave equation, to analyze the growth of harmonic radiation,

$$\left(\frac{\partial^2}{\partial z^2} - \frac{1}{c^2}\frac{\partial^2}{\partial t^2} - \frac{\omega_p^2}{c^2}\right)\vec{E}^{(3)} = \frac{4\pi}{c^2}\frac{\partial\vec{J}^{(3)}}{\partial t}. \quad (24)$$

The procedure to derive the amplitude of the phase mismatched third harmonic involves considering the harmonic field's variationis $\vec{E}^{(3)} = E_3(z)e^{i(k_3 z - 3\omega_0 t)}$ as described by the assumption that $\partial^2 E_3(z)/\partial z^2 << k_3\,\partial E_3(z)/\partial z$. This implies that $\partial E_3(z)/\partial z$ changes in are significantly larger than the wavelength $2\pi/k_3$. Consequently, we can deduce the normalized amplitude for the third harmonic under phase-mismatched conditions

$$E_3 = \frac{-4\pi a_0^2 m^2 c^2 (J_{c3} + J_{s3}) E_0}{\frac{\omega_p^2}{9\omega_0^2}.e\left\{\frac{3\omega_0 m}{n_0 e^2}[J_c(3\omega_0) + J_s(3\omega_0)]-1\right\}} e^{\frac{i\Delta k.z}{2}} \frac{\sin(\Delta k.z/2)}{\Delta k} \quad (25)$$

where, $\Delta k = (k_3 - 3k_0)$ is the wave vector mismatch for third harmonic. The third harmonic conversion efficiency is obtained as

$$\eta_3 = \frac{\mu_3}{\mu_2}\left|\frac{E_3^2}{E_2^2}\right| = \frac{16\pi^2 m^4 c^4 a_0^4 (J_{s3} + J_{c3})^2}{e^2\left(\frac{\omega_p}{3\omega_0}\right)^4 \left\{\frac{3m\omega_0}{n_0 e^2}[J_c(3\omega_0) + J_s(3\omega_0)]-1\right\}^2} \frac{\sin^2(\Delta k.z/2)}{(\Delta k)^2} \quad (26)$$

where,

$$J_s(3\omega_0) = -\frac{2ik_0\mu_B}{\hbar}[n_0 S_{x1} + S_0 n_{x1} + n_0 S_{y1} + S_0 n_{y1} + n_0 S_{z1} + S_0 n_{z1}](3\omega_0)$$

$J_c(3\omega_0) = -en_0[v_{x1} + v_{y1} + v_{z1}](3\omega_0)$ and

$a_0 = eE_0/mc\omega$.

From eq. (26), it is found that the harmonic oscillate in magnitude due to the dephasing between pump laser and the radiation harmonics. The third harmonic radiation is proportional to the plasma electron density, propagation distance and the intensity of laser pulse. The conversion efficiency of third harmonic radiation changes dramatically.

Figure 1 shows the varation of conversion efficiency with propagation distance for intensity around 10^{19} W/cm^2 and frequency $\omega_0 = 1.57\times10^{17}$ s^{-1} for different values of applied magnetic field strength $\omega_c/\omega_0 = 0.03$ for solid and $\omega_c/\omega_0 = 0.05$ for dotted line. The third harmonic conversion efficiency is observed to be periodic with propagation

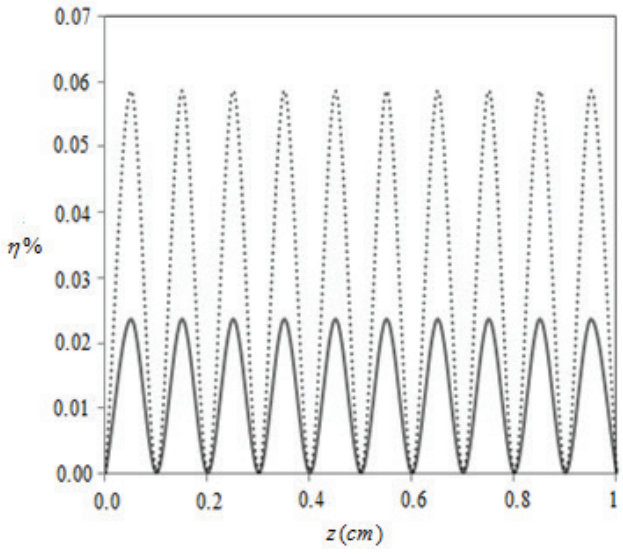

Figure 1. The phase mismatch third harmonic amplitude variation as a function of z/γ for plasma parameters $\omega_p/\omega_0 = 0.3$, $n = 10^{30}$m^{-3}.

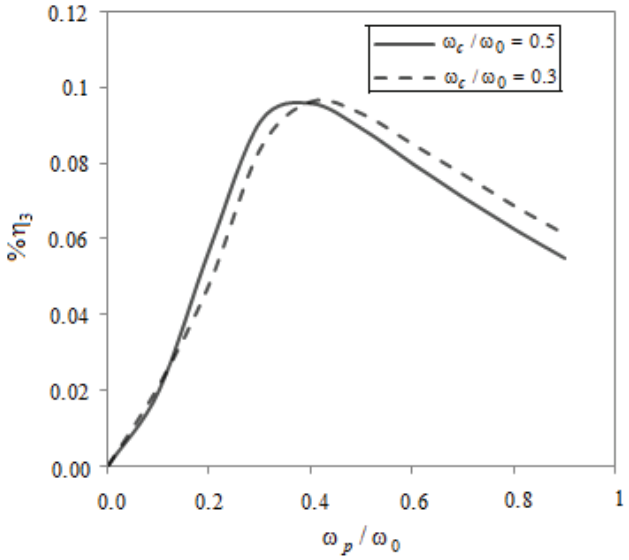

Figure 2. Variation of conversion efficiency as a function of ω_p/ω_0 for, $a_0 = 0.2$ and $n = 10^{30}$m^{-3} and different value of ω_c/ω_0.

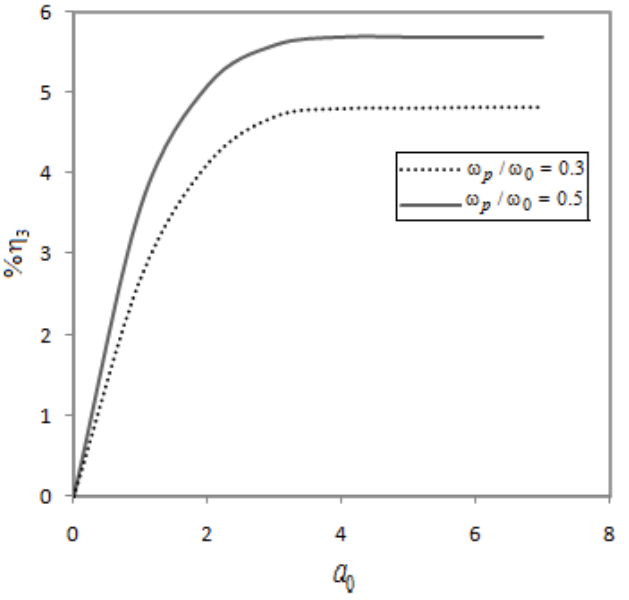

Figure 3. Variation of conversion efficiency against normalized fundamental laser intensity a_0 for various values of ω_p/ω_0.

distance (in pulse frame). The conversion efficiency gets maximum for minmum value of z is given by $z > l'' = \pi/\Delta k$.The length l_c is maximum plasma length upto which third harmonic power increases. For $z > l_c$ the third harmonic efficiency reduces again. The maximum value of η is observed 0.023% for solid line and 0.058% for dotted line after traversing a distance 0.005cm.

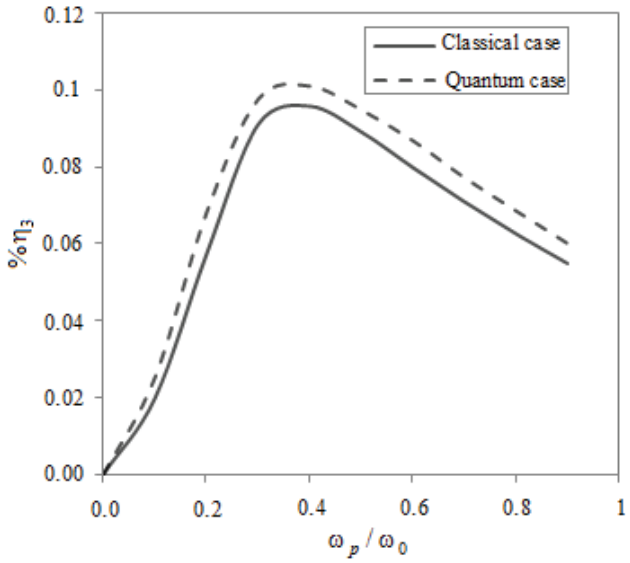

Figure 4. Variation of conversion efficiency as a function of $\omega_p/\omega_{0,}$(i) Solid line in absence of quantum effects and (ii) Dashed line in presence of quantum effects.

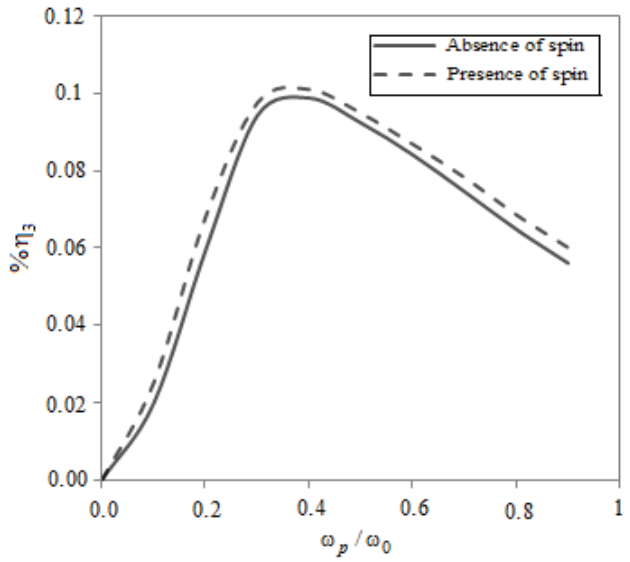

Figure 5. Variation of conversion efficiency as a function of $\omega_p/\omega_{0,}$(i) Solid line in absence of spin effect and (ii) Dashed line in presence of spin effect.

Figure 2 shows the variation in conversion efficiency (η_3%) for the third harmonic with normalized plasma electron density for different values of the intensity of the magnetic field. The graph illustrates how harmonic radiation increases with increasing plasma density until saturation for a constant magnetic field. The applied magnetic field affects the plasma density saturation value, which is higher for weaker magnetic fields.

Third harmonic conversion efficiency varies with laser pulse intensity for various normalized plasma density values, $\omega_p/\omega_0 = 0.3$ for solid and $\omega_p/\omega_0 = 0.5$ for dotted line is ploted in figure 3. It is also noticed that as we increase the intensity of incident laser pulse, third harmonic efficiency increases significantly. It is due to the fact that nonlinear refractive index change due to high intensity results stronger self-focusing which leads to enhance the third harmonic generation. However, at high laser pulse intensities, conversion efficiency becomes saturated.

In Fig. 4, the conversion efficiency of third harmonic radiation in the classical situation is displayed for the following variables: $\omega_c/\omega_0 = 0.3$, $a_0 = 0.2$ and $n = 10^{30}\text{m}^{-3}$. In the limit, the solid line indicates the lack of quantum effects whereas the dotted line indicates the presence of these effects. Due to the existence of quantum effects in magnetoplasma, it is reported that the third harmonic's efficiency is increased by around 12.5%. This is because quantum diffraction effects significantly affect the third harmonic's efficiency of laser pulses.

Figure 5 shows the efficiency of the third harmonic as a function of plasma density. The solid line indicates the absence of the electron spin effect, whereas the dotted line indicates the existence of the electron spin effect. Because electron spin affects plasma current density and introduces correction terms to the harmonic field amplitude, it is reported that the third harmonic's efficiency is around 10% higher due to the existence of spin effects in magnetoplasma.

CONCLUSION

In our study, we examined the outcomes of third harmonic generation resulting from the passage of a circularly polarized laser pulse through a dense quantum magnetoplasma. We aligned a static magnetic field longitudinally to induce magnetization. To comprehend this process, we utilized the recently developed quantum hydrodynamic (QHD) model and employed the self-consistent field approximation for the QHD equations. The impact of various factors, such as Fermi statistical pressure, the quantum Bohm potential and the electrons's spin, were considered. By using perturbative expansion technique, we derived crucial properties like quiver and third-order velocities, electron densities and spin angular momenta. The electron experienced two primary quantum adjustments: one due to density fluctuations and the other due to magnetization energy. These quantum effects, combined with the electron's spin, led to modifications in plasma current density and the harmonic field amplitude. Importantly, quantum diffraction effects contributed to and heightened the production of nonlinear third harmonic radiation. Our findings revealed that third harmonic generation increased with both plasma density and magnetic field strength, up to certain saturation points. Beyond these saturation points, further growth ceased. Notably, an increase in magnetic field strength led

to earlier plasma density saturation, attributed to the polarization field effect in intensely magnetized dense plasma. We also observed that third harmonic radiation efficiency was approximately 12.5% higher in quantum plasma due to the presence of diffraction effects (Bohm potential, spin effect) compared to classical plasma. Additionally, electron spin effects and the absence of quantum diffraction effects contributed to about 10% of the harmonic generation efficiency in quantum plasma. This heightened efficiency could be harnessed as a diagnostic tool to detect the presence of clusters and measure their size during interactions between laser plasma and a gas jet in clustered plasma scenarios.

AUTHORSHIP CONTRIBUTIONS

Authors equally contributed to this work.

DATA AVAILABILITY STATEMENT

The authors confirm that the data that supports the findings of this study are available within the article. Raw data that support the finding of this study are available from the corresponding author, upon reasonable request.

CONFLICT OF INTEREST

The author declared no potential conflicts of interest with respect to the research, authorship, and/or publication of this article.

ETHICS

There are no ethical issues with the publication of this manuscript.

REFERENCES

[1] Gibbon P. High-order harmonic generation in plasmas. IEEE J Quantum Electron 1997;33:1915. [CrossRef]
[2] Goldman L, Seka W, Tanaka K, Short R, Simon A. The use of laser harmonic spectroscopy as a target diagnostic. Can J Phys 1986;64:969. [CrossRef]
[3] Yamanaka C, Yamanka T, Sasaki T, Mizui J, Kang HB. Brillouin backscattering and parametric double resonance in laser-produced plasma. Phys Rev Lett 1974;32:1038. [CrossRef]
[4] Chien JL, Franz XK. The influence of plasma defocusing in high harmonic generation. Opt Express 2011;19:22377. [CrossRef]
[5] Dragila R. Second-harmonic generation at resonance absorption and modified plasma density profile. J Appl Phys 1982;53:865. [CrossRef]
[6] Grebogi C, Tripathi VK, Chen HH. Harmonic generation of radiation in a steep density profile. Phys Fluids 1983;26:1904. [CrossRef]
[7] Lia C, Bundman P, Stegeman GI. Second harmonic generation with surface guided waves in signal processing geometries. J Appl Phys 1983;54:6213. [CrossRef]
[8] Xu Z, Xu Y, Yin G, Z Y, Yu J, Lee P. Second-harmonic emission from laser-plasma interactions. J Appl Phys 1983;54:4902. [CrossRef]
[9] Jha P, Mishra RK, Raj G, Upadhyay A. Second harmonic generation in laser magnetized plasma interaction. Phys Plasmas 2007;14:053107. [CrossRef]
[10] Singh M, Gupta DN. Relativistic third-harmonic generation of a laser in a self-sustained magnetized plasma channel. IEEE J Quantum Electron. 2014;50:491. [CrossRef]
[11] Wadhwani N, Kumar P, Jha P. Nonlinear theory of propagation of intense laser pulses in magnetized plasma. Phys Plasmas 2002;9:263. [CrossRef]
[12] Wilks SC, Kruer WL, Mori WB. Odd harmonic generation of ultra-intense laser pulses reflected from an overdense plasma. IEEE Trans Plasma Sci 1993;21:120. [CrossRef]
[13] Esarey E, Ting A, Sprangle P, Umstadter D, Liu X. Nonlinear analysis of relativistic harmonic generation by intense lasers in plasmas. IEEE Trans Plasma Sci 1993;21:95. [CrossRef]
[14] Dromey B, Zepf M, Gopal A, Lancaster K, Wei MS, Krushelnick K, et al. High harmonic generation in the relativistic limit. Nat Phys 2006;2:456. [CrossRef]
[15] Banerjee S, Valenzuela AR, Shah RC, Maksimchuk A, Umstadter D. High harmonic generation in relativistic laser-plasma interactions. Phys Plasmas 2002;9:2393. [CrossRef]
[16] Singh RP, Gupta SL, Thareja RK. Third harmonic generation in air ambient and laser ablated carbon plasma. Phys Plasmas 2015;22:123302. [CrossRef]
[17] Rax JM, Fisch NJ. Phase-matched third harmonic generation in a plasma. IEEE Trans Plasma Sci 1993;21:105. [CrossRef]
[18] Liu T, Xiao S, Li B, Gu M, Luan H, Fang X. Third- and second-harmonic generation in all-dielectric nanostructures. Front Nanotechnol 2022;4:891892. [CrossRef]
[19] Magnus W, Schoemaker W. Quantum transport in submicron devices: a theoretical introduction. Berlin, Heidelberg: Springer; 2002. [CrossRef]
[20] Lai D. Matter in strong magnetic fields. Rev Mod Phys 2001;73:629. [CrossRef]
[21] Opher M, Silval O, Dauger DE, Decyk VK, Dawson JM. Nuclear reaction rates and energy in stellar plasmas: the effect of highly damped modes. Phys Plasmas 2001;8:2454. [CrossRef]
[22] Chabrier G, Douchin F, Potekhin AY. Dense astrophysical plasmas. J Phys Condens Matter 2002;14:9133. [CrossRef]
[23] Sarkar J, Chandra S, Goswami J, Das C, Ghosh B. Growth of RT instability at the accreting magnetospheric boundary of neutron stars. AIP Conf Proc 2021;2319:030006. [CrossRef]
[24] Chandra S, Goswami J, Sarkar J, Das C, Nandi D, Ghosh B. Formation of electron acoustic shock wave in inner magnetospheric plasma. Indian J Phys 2022;96:3413–3427. [CrossRef]

[25] Manfredi G, Fexi MR. Theory and simulation of classical and quantum echoes. Phys Rev E 1996;53:6460. [CrossRef]

[26] Piovella N, Cola MM, Volpe L, Schiavi A, Bonifacio R. Three-dimensional Wigner-function description of the quantum free-electron laser. Phys Rev Lett 2008;100:044801. [CrossRef]

[27] Malkin VM, Fisch NJ, Wurtele JS. Compression of powerful x-ray pulses to attosecond durations by stimulated Raman backscattering in plasmas. Phys Rev E 2007;75:026404. [CrossRef]

[28] Hartemann FV, Siders CW, Barty CPJ. Theory of Compton scattering in ignited thermonuclear plasma. J Opt Soc Am B 2008;25:167. [CrossRef]

[29] Sarkar J, Chandra S, Dey A, Das C, Marick A, Chatterjee P. Forced KdV and envelope soliton in magnetoplasma with kappa distributed ions. IEEE Trans Plasma Sci 2022;50:1565–1578. [CrossRef]

[30] Sharry, Dutta D, Ghosh M, Chandra S. Magnetosonic shocks and solitons in Fermi plasma with quasiperiodic perturbation. IEEE Trans Plasma Sci 2022;50:1585–1597. [CrossRef]

[31] Singla S, Chandra S, Saini NS. Simulation study of dust magnetosonic excitations in a magnetized dusty plasma. Chin J Phys 2023;85:524–533. [CrossRef]

[32] Gupta N, Singh A. Dynamics of quadruple laser pulses in under-dense plasmas. Contrib Plasma Phys 2017;57:258. [CrossRef]

[33] Kumar P, Singh S, Ahmad N. Conversion efficiency of even harmonics of whistler pulse in quantum magnetoplasma. Laser Part Beams 2019;37:5. [CrossRef]

[34] Kumar P, Singh S, Singh AK. Harmonic generation in magnetized quantum plasma. AIP Conf Proc 2016;1728:020173. [CrossRef]

[35] Das C, Chandra S, Ghosh B. Effects of exchange symmetry and quantum diffraction on amplitude modulated electrostatic waves in quantum magnetoplasma. Pramana J Phys 2021;95:78. [CrossRef]

[36] Thakur S, Das C, Chandra S. Stationary structures in a four-component dense magnetoplasma with lateral perturbations. IEEE Trans Plasma Sci 2022;50:1545–1556. [CrossRef]

[37] Rathore NS, Kumar P. Phase-matched third harmonic generation of a Gaussian laser pulse in high-density quantum plasma. Am J Mod Phys 2016;5:154. [CrossRef]

[38] Shukla PK, Eliasson B. Nonlinear aspects of quantum plasma. Phys Usp Fiz Nauk 2010;180:55. [CrossRef]

[39] Shukla PK, Ali S, Stenflo L, Marklund M. Nonlinear wave interactions in quantum magnetoplasmas. Phys Plasmas 2006;13:112111. [CrossRef]

[40] Misra AP, Brodin G, Marklund M, Shukla PK. Localized whistlers in magnetized spin quantum plasmas. Phys Rev E 2010;82:056406. [CrossRef]